A unique variant of lymphocytic choriomeningitis virus that induces pheromone binding protein MUP: Critical role for CTL

Brian C. Ware[a,1], Brian M. Sullivan[a,1], Stephanie LaVergne[a], Brett S. Marro[a], Toru Egashira[b,c,d,e], Kevin P. Campbell[b,c,d,e], John Elder[f], and Michael B. A. Oldstone[a,2]

[a]Viral-Immunobiology Laboratory, Department of Immunology and Microbiology, The Scripps Research Institute, La Jolla, CA 92037; [b]Department of Molecular Physiology, Roy J. and Lucille A. Carver College of Medicine, University of Iowa, Iowa City, IA 52242; [c]Department of Biophysics, Roy J. and Lucille A. Carver College of Medicine, University of Iowa, Iowa City, IA 52242; [d]Department of Neurology, Roy J. and Lucille A. Carver College of Medicine, University of Iowa, Iowa City, IA 52242; [e]Howard Hughes Medical Institute, Roy J. and Lucille A. Carver College of Medicine, University of Iowa, Iowa City, IA 52242; and [f]Department of Immunology and Microbiology, The Scripps Research Institute, La Jolla, CA 92037

Contributed by Michael B. A. Oldstone, July 8, 2019 (sent for review April 25, 2019; reviewed by Esteban Domingo and Allan J. Zajac)

Lymphocytic choriomeningitis virus (LCMV) WE variant 2.2 (v2.2) generated a high level of the major mouse urinary protein: MUP. Mice infected with LCMV WE v54, which differed from v2.2 by a single amino acid in the viral glycoprotein, failed to generate MUP above baseline levels found in uninfected controls. Variant 54 bound at 2.5 logs higher affinity to the LCMV receptor α-dystroglycan (α-DG) than v2.2 and entered α-DG–expressing but not α-DG–null cells. Variant 2.2 infected both α-DG–null or –expressing cells. Variant 54 infected more dendritic cells, generated a negligible CD8 T cell response, and caused a persistent infection, while v2.2 generated cytotoxic T lymphocytes (CTLs) and cleared virus within 10 days. By 20 days postinfection and through the 80-day observation period, significantly higher amounts of MUP were found in v2.2-infected mice. Production of MUP was dependent on virus-specific CTL as deletion of such cells aborted MUP production. Furthermore, MUP production was not elevated in v2.2 persistently infected mice unless virus was cleared following transfer of virus-specific CTL.

pheromones | MUP | cytotoxic T lymphocytes (CTL) | lymphocytic choriomeningitis virus (LCMV)

Here we evaluated biological and chemical differences between 2 variants, v2.2 and v54, obtained from the WE strain (1, 2) of lymphocytic choriomeningitis virus (LCMV). Earlier we documented that the parental WE strain was unable to infect growth hormone (GH) -producing cells located within the anterior lobe of the pituitary gland of C3H/St mice. However, the quasispecies analysis of the parental WE strain revealed variants infectious for such cells. After plaque-purifying 61 clones from the parental WE strain, we documented that 58 of 61 clones (95%) including v54 had the phenotype of the parental WE master strain and failed to infect GH cells in vivo. In contrast, 3 of 61 WE clones (5%), like v2.2, robustly infected such GH-producing cells (3–5).

The LCMV genome consists of 2 RNA segments that encode proteins from the 4 genes, 2 on a short (S) piece of RNA (5′ glycoprotein, nucleoprotein) and 2 on the long (L) piece of RNA (5′ Z, polymerase) (reviewed in ref. 6). Reassortants between Armstrong (ARM) and WE localized the GH infection phenotype only to genes on the S RNA (7). The NP sequence is identical for WE and ARM. However, on the GP there was 1 amino acid difference, located at amino acid residue 260 WE/ARM: Leu/Phe. Both v54 and v2.2 had Leu at GP residue 260 but differed by a single amino acid at residue GP 153: v54, Ser; v2.2, Phe.

We report studies examining the binding, cell entry, tropism, immune, and mouse urinary protein (MUP) production differences between v2.2 or v54. MUPs belong to a family of proteins known as lipocalins. Their 8 β-sheets arranged as a β-barrel open at one end, with α-helices at both amino- and carboxyl-termini forming a ligand binding pocket. The pocket can accommodate specific small chemical molecules (pheromones). MUPs can also act themselves as protein pheromones. Pheromones are specific chemical signals, important for communication between individuals of the same species. Pheromones are used to coordinate multiple aspects of social behavior, including geographic boundary limits, sexual recognition, and attraction for bringing opposite sexmates together for mating (8, 9).

Variant 54 infected significantly more splenic conventional dendritic cells (cDCs) and plasmacytoid (p)DCs than did v2.2. DCs were previously shown to be central in the pathogenesis of persistent LCMV infection (10–12). Variant 54 generated a meager virus-specific CD8 and CD4 T cell response compared to v2.2 and was unable to clear an acute viral infection. In contrast, the virus-specific T cell response generated by v2.2 was vigorous and successfully terminated the acute LCMV infection. Importantly, MUP was shown to be induced during viral infection. MUP appeared in significantly higher levels in urine from mice infected with v2.2. In contrast, MUP levels were minimal and equivalent in v54-infected and noninfected controls. $CD8^+$ T cells played an essential role as deletion of CD8 T cells aborted MUP production in v2.2-infected mice. Furthermore, persistent v2.2 infection was not associated with enhanced MUP levels. However, when such mice had a restoration of functional virus-specific cytotoxic T lymphocytes (CTL), infection was curtailed and significant elevation of MUP occurred.

Significance

Pheromones play essential roles in host communications and sexual attraction, and thus regulate adaptive behavior. Here we present the discovery and characterization of the first known virus, a variant of lymphocytic choriomeningitis virus, that selectively induces pheromone binding protein mouse urinary protein. Furthermore, we found that cytotoxic T lymphocytes play a critical role in mouse urinary protein generation.

Author contributions: B.C.W., J.E., and M.B.A.O. designed research; B.C.W., B.M.S., S.L., B.S.M., and J.E. performed research; T.E. and K.P.C. contributed new reagents/analytic tools; and M.B.A.O. wrote the paper.

Reviewers: E.D., Spanish Research Council; and A.J.Z., University of Alabama at Birmingham.

The authors declare no conflict of interest.

[1]B.C.W. and B.M.S. contributed equally to this work.

[2]To whom correspondence may be addressed. Email: mbaobo@scripps.edu.

This article contains supporting information online at www.pnas.org/lookup/suppl/doi:10.1073/pnas.1907070116/-/DCSupplemental.

Published online August 19, 2019.

Results and Discussion

All experiments had a minimum of 4 mice per group, frequently 5 to 10 mice, except for MUP studies that used 10 to 20 mice per group. Experiments were repeated at least twice, usually 4 times.

Compared to v2.2, v54 Binds at Significantly Higher Affinity to the LCMV Cellular Receptor α-DG and Only Infects Cells Expressing α-DG. In the first series of experiments we compared the binding of v54 and v2.2 to the LCMV receptor α-dystroglycan (α-DG) (11, 13–17). Two assays, a virus overlay protein blot assay (13, 15, 16) and ELISA using purified α-DG (13, 14) both indicated the significant binding of v54 by 2 logs or more over v2.2 (Fig. 1 *A* and *B*). Variant 54 was able to infect embryonic stem cell (ESC) R1 that expressed α-DG on its surface but not ESC B11 α-DG–null cells (Fig. 1 *C–E*). Utilizing flow cytometry, quantitation for binding v54 or v2.2 to α-DG–null or –expressing cells is shown in Fig. 2. When ESC B11 α-DG–null cells were transfected with a gene expressing α-DG, they now expressed α-DG and infection with v54 occurred. In contrast, v2.2 easily infected ESC B11 α-DG–null and ES cells R1 that expressed α-DG (Figs. 1 *C–E* and 2). Previous genetic reassorting experiments indicated that genes on the S RNA and proteins they encode were responsible for α-DG binding (14, 16, 17). Of those proteins, the NP sequence is identical for v54 and v2.2 but the GP showed a single amino acid difference v54/v2.2: 153 Ser/Phe. These findings suggest v54, which contained the small aliphatic amino acid Ser at GP residue 153, was able to fit into α-DG receptor binding site (14, 17), while v2.2 containing the bulky aromatic Phe in this position was not. Since v2.2 infected α-DG–null and α-DG–expressing cells equally (Fig. 1*E*), it likely utilized an additional cell surface receptor other than α-DG to enter ESCs.

DCs Are Preferentially Infected with v54 and Not v2.2. Among cells of the immune system, DCs express by far the greatest amount (>98%) of α-DG (11, 15). Therefore, we determined if in vivo cDCs and pDCs were more abundantly infected with v54 than v2.2. Purification of these 2 populations of DCs was performed using known markers from spleens of immunocompetent C57BL/6 adult mice at 7, 15, and 30 d postinfection with the 2 variant viruses. As shown in Table 1, 3-fold or more cDCs were infected by v54 compared to v2.2 at days 7, 15, and 30 postinfection. Similarly, 3-fold or more pDCs were infected at days 7 and 15 postinfection by v54 compared to v2.2. Kinetics of infection of cDCs by v54 indicated few cells were infected by day 7 with peak

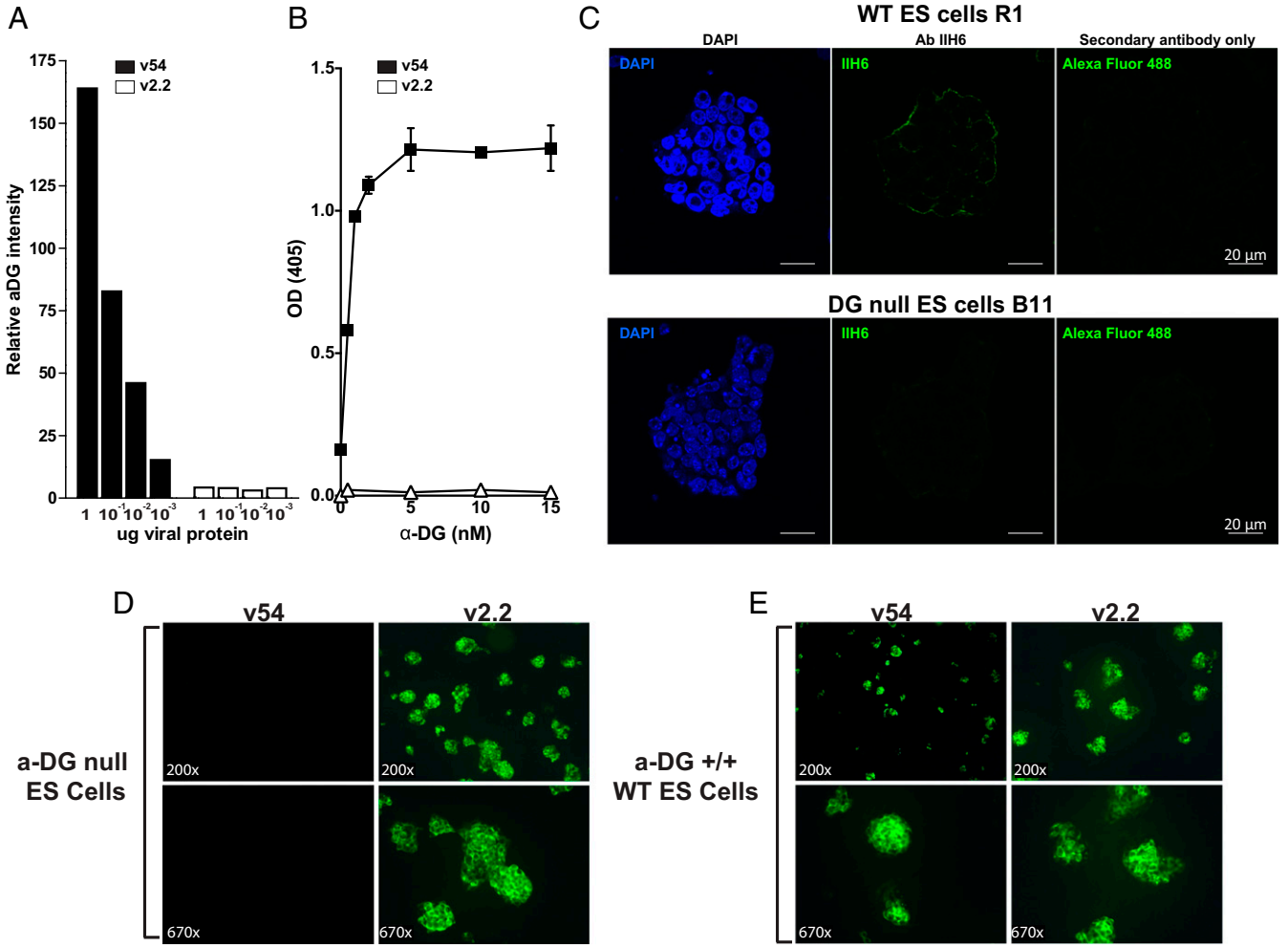

Fig. 1. Binding of v54 or v2.2 viruses to purified α-DG and entry into ESC that failed to express or expressed α-DG. (*A*) Binding of v54 or v2.2 to purified α-DG in a virus overlay protein blot assay. Data shown are quantitated to microgram of viral protein bound. (*B*) Binding of v54 or v2.2 to soluble DG fused to the Fc region of human IgG using an ELISA. (*C*) ESCs that expressed α-DG (R1) or failed to express α-DG (B11). Primary strains with monoclonal antibody IIH-6 specific for α-DG followed by secondary fluoresceinated antibody to mouse IgM. The *Right* panel indicates the secondary antibody control. (*D*) Display of v54 or v2.2 single-cycle infection (12 h) of α-DG null (B11) cells. Note inability of v54 to infect such cells while v2.2 can. Stain used was monoclonal antibody (VL4) to the viral NP whose sequence is identical for v54 and v2.2. (*E*) v54 and v2.2 both infected ESCs (R1) that had α-DG on their surfaces.

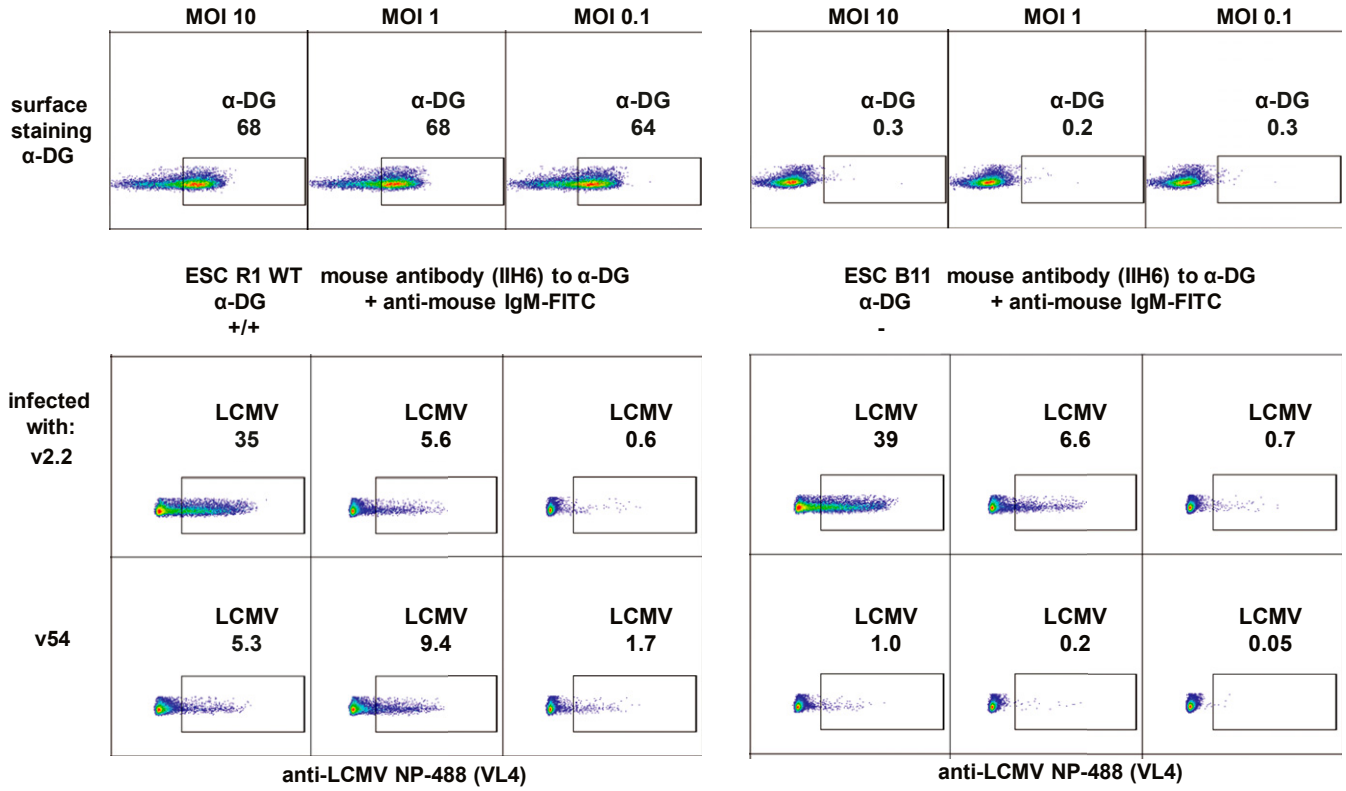

Fig. 2. Quantitation of viral NP in α-DG–null (B11) or α-DG$^+$ (R1) cells using antibody to viral NP (VL4) and FACS.

levels at days 15 and 30, while in contrast pDCs infected with v54 were greater than v2.2 at day 7, peaked at day 15, and by day 30 returned to levels seen with v2.2 (Table 1).

We previously showed that LCMV Cl 13, a variant obtained from ARM 53b in vivo by lymphoid tissue selection (11, 18) bound at 2 to 2.5 logs higher affinity to α-DG and infected significantly more cDCs in vivo (11, 12, 15) than the parental ARM 53b. We then used Cl 13 and ARM, respectively, as positive and negative controls (10–12, 17–19) for infection of DCs, generation of CTL, and resultant clearance or persistent infection following challenge with 2×10^6 PFU intravenously of v54 and v2.2 (Tables 2 and 3).

Variant 54 Fails to Elicit a Virus-Specific CD8 T Cell Response While v2.2 Generates a Robust MHC-Restricted CD8 T Cell Response in Both Immunocompetent C57BL/6 (H-2b) and Balb/cdj (H-2d) Mice. To test for the generation of a robust CTL response, 2×10^6 PFU of the various viruses listed in Table 2 were given intravenously to immunocompetent 8-wk-old C57BL/6 and Balb/cdj mice. After 7 d of infection, spleens were removed, and single-cell suspension of lymphocytes obtained (17, 18) and added to ^{51}Cr-labeled H-2b or H-2d targets at effector to target ratios of 50 or 25:1 (17, 18). Six hours later cell-free supernatants were obtained and the ^{51}Cr counts quantified. As shown in Table 2 in an MHC-restricted CTL assay, while v2.2 and ARM 53b generated a robust CTL response in both C57BL/6 (H-2b) and Balb/cdj (H-2d) mice, neither v54 nor Cl 13 did.

We then analyzed the generation of v54, v2.2, Cl 13, and ARM 53b splenic CD8 CTL and CD4 T cells to known immunodominant T cell epitopes of C57BL/6 H-2b mice. The D^b-restricted CD8 T cell epitopes are associated with GP 33–41, GP 276–284, and NP 396–403. As seen in Fig. 3, v2.2 and ARM 53b both generated robust CD8 T cells to these 3 epitopes. In contrast, v54 and Cl 13 generated weak to negligible CD8 T cell responses. A surprise was the smaller response with v2.2 in eliciting GP 276–284 and NP 396–403 CTL compared to response of ARM 53b, although as anticipated both GP 276–284 and NP 396–403 responses were significantly more robust following v2.2 infection compared to infection with v54. At day 7 postinfection, a more robust CD4 T cell response was made by v2.2 and ARM 53b when compared to responses made by v54 and Cl 13, respectively. The virus-specific CD4 T cell response, as anticipated, was

Table 1. Viral antigen expression in dendritic cells

Virus	cDCs (CD11c$^+$, MHCII$^+$, B220nil, F4/80 low)			pDCs (PDCA$^+$, SiglecH$^+$, CD11c low, B220$^+$)		
Virus	d7	d15	d30	d7	d15	d30
v54	3*	34	30	9	28	8
v2.2	<1	9	6	<1	9	8
Cl13	ND	26	ND	ND	36	ND
ARM53b	ND	<1	ND	ND	4	ND

This table shows presence of LCMV NP antigen kinetically in cDCs and pDCs over 30 d postviral infection. ND, not done.
*Percent of cells expressing LCMV NP by FACS

Table 2. Percent of ^{51}Cr released by target cells infected with various viruses

Mice infected with:		MC57 (H-2b target)		Balb (H-2d target)	
C57BL/6 (H-2b)	E:T	50:1	25:1	50:1	25:1
v54		10*	1	4	2
v2.2		35	16	2	2
Cl13		3	<1	1	<1
ARM53b		60	53	4	3
Balb/cdj (H-2d)	E:T	50:1	25:1	50:1	25:1
v54		4	2	3	2
v2.2		5	1	43	21
Cl13		3	1	5	4
ARM53b		2	3	34	26

This table demonstrates that v54 is unable to generate a robust CTL response while v2.2 can. Used is an MHC-restricted virus-specific CD8 T cell ^{51}Cr assay 7 d following virus infection. E:T, effector:target ratio.
*Specific ^{51}Cr release, samples done in triplicate.

lower than the corresponding CD8 T cell response at the time sampled.

Variant 54 Causes a Persistent Virus Infection While v2.2 Is Cleared in Sera and Tissues Except for Kidney 15 d Postinfection. A robust CD8 T cell response alone is required and sufficient to clear an acute virus infection by 15 d postinfection (11, 19–23). In contrast, both virus-specific CD8 and CD4 T cells are required to prevent a persistent infection (19, 21, 22). From the data in Table 2 and Fig. 3, we expected following v2.2 and ARM 53b infection the acute viral infection would be terminated. Table 3 and *SI Appendix*, Table S1 show this to be the case except for kidneys, where virus persisted 73 d (latest time-point studied) postinfection. Correspondingly, since neither v54 nor Cl 13 generated robust CD8 or CD4 virus-specific T cell responses, a persistent infection was expected and occurred in all mice over the 73-d observation period.

Urine of C57BL/6 Mice Infected with v2.2 Contains Significantly More Pheromone (MUP) than Infection with v54. MUP is transcribed in the liver and then transported to the circulation and to the kidney. While the total function of MUP is not completely clear, there is evidence MUP serves as the major murine pheromone transport protein for communication between mice and for sexual attraction (8, 9, 24). As virus persisted in kidneys of v2.2- and v54-infected C57BL/6 mice, we evaluated whether or not there was evidence of proteins or virus in the urine of these mice. Using primarily males, we found no evidence of either infectious virus or large proteins like albumin in their urine (Fig. 4 *A*–*C*). However, low molecular weight MUP occurred in the urine as expected in noninfected controls and in both v2.2- and v54-infected mice (Fig. 4 *B* and *C*). Unexpected was the significantly larger amounts of MUP in v2.2-infected mouse urine at 20 d (Fig. 4*A*) that peaked at 30 d postinfection when compared to v54-infected or noninfected control mice (Fig. 4 *B* and *C*) ($P \leq 0.0001$). Levels of significantly elevated MUP in urine of C57BL/6 males infected with v2.2 was detected 40 d postinfection. In contrast, MUP in the urine of v54-infected mice was not enhanced over MUP titers in age-matched noninfected controls (Fig. 4 *B* and *C*). Virus was cleared from sera, liver, and brain (Table 3) in infected v2.2 mice but persisted in v54-infected mice up to the last observation point at day 73 postinfection. Virus was found in kidneys of all mice infected with v2.2 or v54 but not in their urine at days 15 through 73 after virus inoculation (Table 3 and *SI Appendix*, Table S1). There was no histologic evidence of injury to the glomeruli, proximal or distal tubules in v2.2-infected mice sampled kinetically at days 6/7, 15, 30, 45, and 73 postinitiation of infection. MUP was identified by Western blot and use of specific antibodies (24) (Fig. 4). Presence of MUP, but no larger serum proteins such as albumin (Fig. 4*B*), in the urine of v2.2-infected mice is consistent with preserved integrity of the renal glomerular membrane where injury would lead to release of large molecules in the urine. There was minimal expression of MUP from v54-infected mice, indicating the ability of renal tubules to reabsorb most MUP and other low-weight proteins back to the circulation (Fig. 4 *B* and *E*, *Bottom Right*). The presence of large amounts of the low molecular weight MUP protein in v2.2-infected mouse tubules and urine suggested that there may likely be a specific mechanism in the tubules that preferentially blocks MUP reabsorption and favors pheromone secretion in the urine (Fig. 4 *B*, *C*, and *E*, *Bottom Left*).

We evaluated the amounts of MUP RNA and protein to determine whether MUP was transcribed in the kidney as well as the liver in v2.2- and v54-infected mice. Using qPCR, we noted transcription of MUP occurred in the livers of both v2.2- and v54-infected mice and not in their kidneys (Fig. 4*D*). Transcription of MUP in v2.2 mice was significantly greater (7- to 8-fold enhanced) than that observed with v54 (Fig. 4*D*). Counting MUP-expressing cells (Fig. 4*E*) located around over 100 positive ductal structures indicated that >75% of hepatocytes from v2.2 mice were positive compared to <30% from v54 mice. Fig. 4*E* shows that by immunohistochemistry the presence of MUP (Fig. 4*E*, green color) was limited to liver hepatocytes. Low-power (2×) confocal microscopy (Fig. 4 *E*, *Top Left*) showed concentration of MUP by ductal cells. Staining of DCs ($CD11c^+$, $MHCII^+$, CD11bnil stain), Kupffer cells ($F4/80^+$, $CD11b^+$ stain), or endothelial cells ($CD31^+$ stain) failed to show presence of MUP (Fig. 5 *A* and *B*), indicating MUP resided in hepatocytes (Figs. 4*E* and 5*A*) and not in DCs, Kupffer cells, or endothelial cells. Minimal liver damage was observed at days 3, 6, 15, or 30 after v2.2 inoculation. Areas of necrosis were few and spotty. Cells of sinusoids, Kupffer, and endothelial cells at days 3, 6, and 15 appeared enlarged, indicating reactivity of these cells in the sinusoids. Increased infiltration of T cells were noted primarily at days 5 to 7 after v2.2 inoculation. Thereafter, levels of virus-specific CD8 T cells remained but were diminished in numbers in the liver parenchyma. Their quantitation over the observation period of days 3, 6, 15, and 30 is shown in *SI Appendix*, Fig. S1. Over this time, serum levels of alanine amino transferase (ALT) were only minimally to modestly elevated (2.1 U/L less fold over age- and sex-matched controls, 10 mice per time) (Fig. 4*A*), confirming the lack of hepatic injury. By comparison, during severe hepatitis ALT was enhanced 7- to 10-fold. The number of hepatocytes (MUP^+), endothelial cells, Kupffer cells, and DCs

Table 3. Virus titers following 2×10^6 PFU intravenous challenge

Day postinfection	Virus	Sera	Kidney	Liver	Brain
d7	v54	4×10^5*	3×10^8	5×10^7	7×10^6
	v2.2	3×10^3	5×10^3	3×10^3	4×10^3
	Cl13	4×10^5	7×10^4	1×10^5	6×10^4
	ARM53b	1×10^2	8×10^1	2×10^2	3×10^2
d15	v54	7×10^4	2×10^6	ND	ND
	v2.2	Nil	5×10^3	ND	ND
	Cl13	4×10^5	5×10^5	ND	ND
	ARM53b	Nil	2×10^3	ND	ND
d73	v54	2×10^4	5×10^4	5×10^3	8×10^3
	v2.2	Nil	1×10^3	Nil	Nil
	Cl13	4×10^5	3×10^4	5×10^3	7×10^3
	ARM53b	Nil	2×10^2	Nil	Nil

This table displays by plaque assay the amount of infection virus in sera and tissues cleared over time following 2×10^6 PFU intravenous challenge with viruses. ND, not done; Nil, $<1 \times 10^2$.
*Mean for 4 to 5 mice per group.

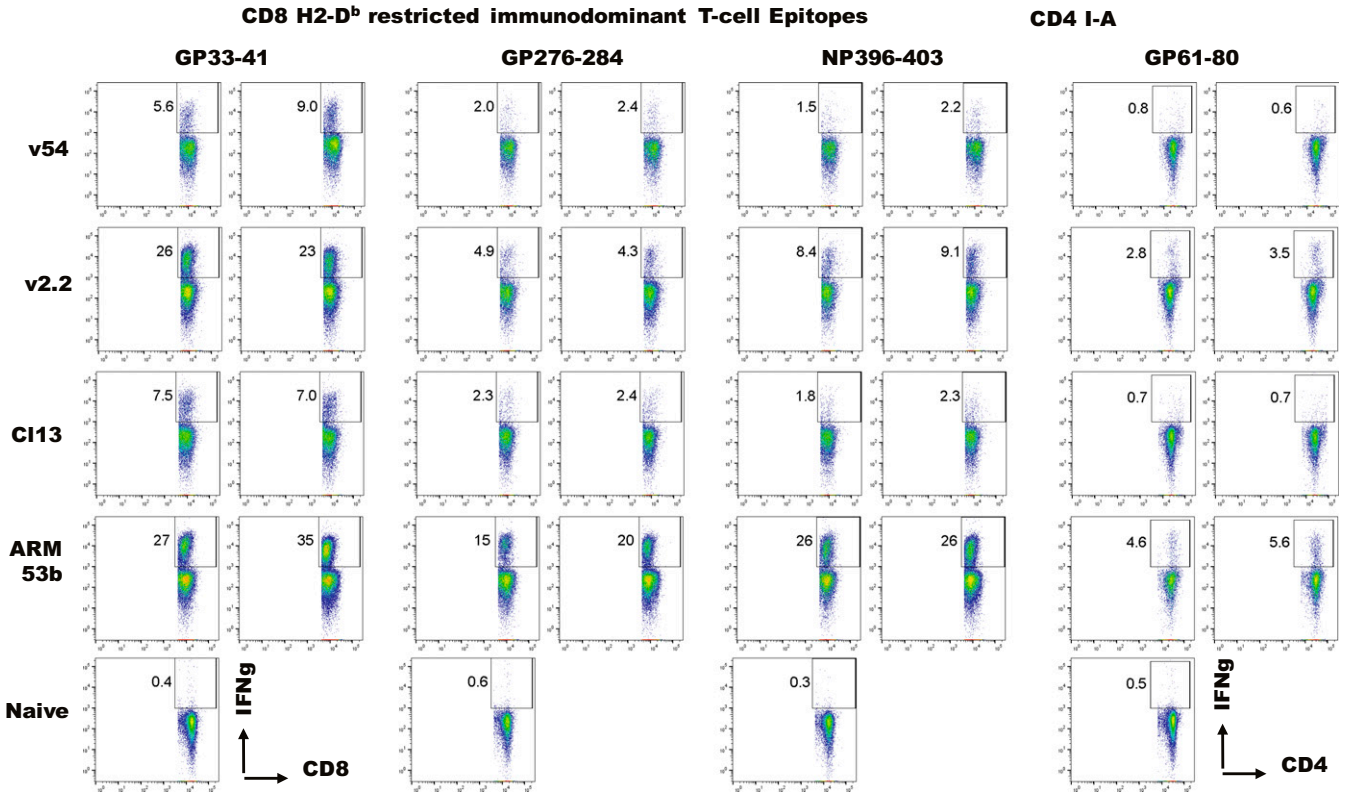

Fig. 3. Quantitation of virus-specific CD8 or CD4 splenic T cell responses at 7 d following v54, v2.2, Cl 13, or ARM 53b infection. Virus-specific peptides to all major immunodominant CD8 and CD4 T cell epitopes were used.

isolated from v2.2 or ARM-infected or uninfected (naïve) livers was comparable (Fig. 5 *B*, *Left*). In contrast, LCMV NP and GP antigen at day 6 (Fig. 5 *A* and *B*, *Right*) was not expressed in hepatocytes but resided primarily in Kupffer cells (Fig. 5 *A*, *Top Left*; Fig. 5 *B*, *Right*) and to a lesser degree DCs and endothelial cells (Fig. 5 *A*, *Right*). By day 30 after v2.2 inoculation, <10% of Kupffer cells expressed viral antigen.

Infection with v2.2 elicited a robust $CD8^+$ CTL response associated with clearance of the acute viral infection (Fig. 3 and Tables 2 and 3). When CD8 CTL were deleted from v2.2-infected mice using a monoclonal antibody, significantly less MUP was made in the urine (Fig. 5*C*). As anticipated, deletion of CD8 CTL from v54 persistently infected mice had no significant effect in MUP production (Fig. 5*C*). Mice infected at birth with v2.2 develop a lifelong persistent viral infection (11, 18, 19) (Fig. 5*D*). MUP levels were not elevated in v2.2 persistently infected adult mice unless they received functional CTL obtained via adoptive transfer of 2×10^7 immune memory T cells (11, 19) (Fig. 5*D*). Thus, CTLs played an essential role in MUP production.

We determined whether the enhanced MUP found in urine was a general phenomenon with additional strains of mice infected with v2.2 and also infection with ARM 53b and Cl 13 viruses. We found the FVB/N (H-2q) mice showed significant enhancement of MUP in urine, as did C57BL/6 (H-2b) mice (Fig. 5*E*) at 30-d after v2.2 infection. Balb/cdj (H-2d) mice expressed less MUP in their urine and there was no significant difference in MUP made in Balb/cdj mice compared to non-infected Balb/cdj controls or following v54 infection (Fig. 5*E*). The ARM 53b strain of LCMV has similar biologic phenotypes to v2.2. Both negligibly bind to the α-DG receptor, have equal entry into α-DG–null and –expressing cells (Figs. 1 and 2), infect limited numbers of DCs (Table 1), and generate a robust virus-specific T cell response (Fig. 3 and Table 2). While there was significant enhancement of MUP urinary levels in FVB/N (H-2q) mice as in C57BL/6 (H-2b) mice infected with v2.2 (Fig. 5*E*), infection by ARM 53b in either C57BL/6 or FVB/N mice did not significantly enhance urinary MUP levels (Fig. 5*F*). Infection with Cl 13 has a phenotype like v54 (Fig. 3 and Table 1) and showed negligible increase in urinary MUP (Fig. 5*F*). Surprisingly, there was no significant difference in enhanced MUP levels following infection with either Cl 13 or ARM 53b (Fig. 5*F*).

Finally, we utilized chimeric viruses where GP of v2.2 or of v54 was placed on the backbone of Cl 13 (containing Cl 13 NP, Z, and L genes). When these viruses, GP v2.2/Cl 13 and GP v54/Cl 13, were employed to infect C57BL/6 mice, infection with GP v2.2 but not GP v54 led to enhanced production of MUP (Fig. 5*F*). These results indicate that the Phe in GP v2.2 at residue 153 played an important role in the excessive production of the pheromone.

In conclusion, variant viruses isolated from a quasispecies of a parental virus provided dramatically different biologic outcomes, a "wolf in sheep's clothing." This phenomenon, reported here for v2.2 and v54 on a single point mutation (GP residue 153 v2.2/v54: Phe/Ser), led to important and diverse changes in the biology of these 2 variants (Figs. 1–5 and Tables 1–3). Quasispecies containing variants, which on the basis of a single amino acid showed biologic differences, have been documented for other RNA viruses from multiple families (25–32).

Variant 54 uses α-DG as the cellular receptor and cell entry factor leading to infection of DC and virus persistence (Figs. 1–3 and Table 1), observations that parallel infections with Cl 13, LCMV Traub, and parental WE (11, 16). In contrast, neither v2.2 nor ARM 53b depend on α-DG for binding and cell entry, and infected both α-DG–expressing and α-DG–null cells. An alternative receptor for α-DG had been observed for ARM 53b (33) and may be used for v2.2.

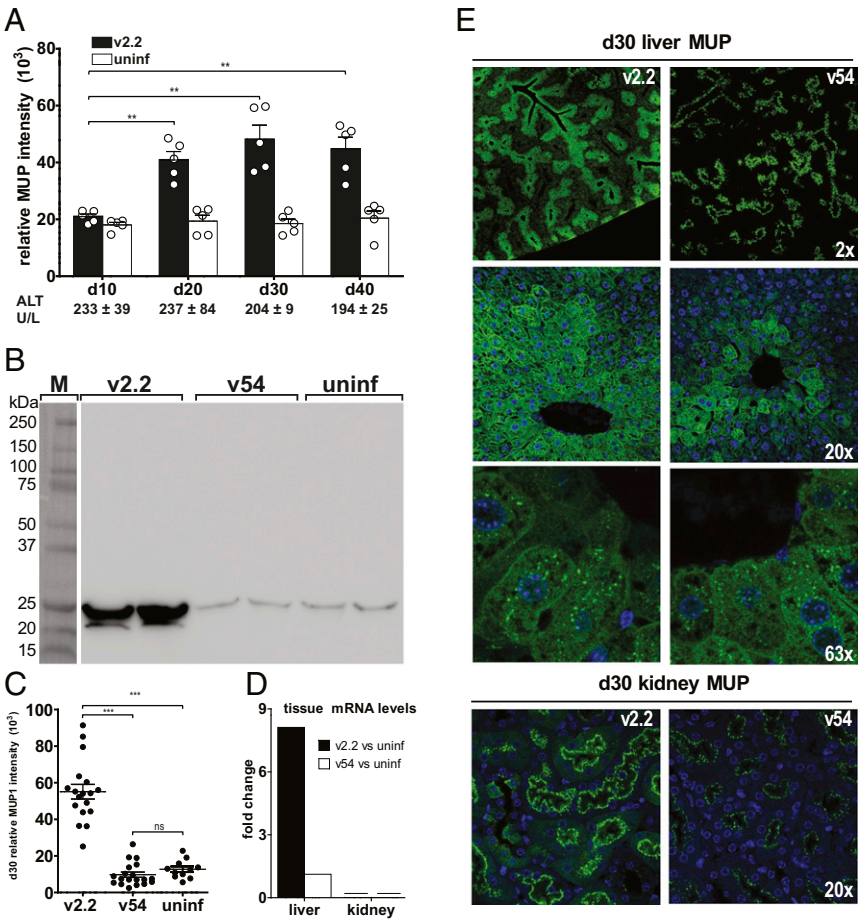

Fig. 4. Expression of significantly larger amounts of MUP in urine of C57BL/6 mice following infection with v2.2 compared to those infected with v54 or to uninfected mice. (*A*) Kinetics of MUP expression in the urine following infection with 2×10^6 PFU of v2.2. Significance is $^{**}P < 0.001$. Each dot records a value for a mouse. At each time displayed, serum levels of ALT (U/L) were measured in livers of v2.2-infected mice. These levels were 2.1-fold or less than measure of ALT in uninfected mice (10 mice per group). In contrast, mice with fulminating hepatitis (positive control) had measurements 7- to 10-fold higher. (*B*) Western blot showing the presence of MUP and no other protein in the urines of C57BL/6 male mice at day 30 after v2.2 infection. (*C*) Each dot represented an individual mouse's value. Note: urine from male C57BL/6 mice 30 d after v54 infection or of uninfected controls possessed equivalent low levels of MUP. Differences between higher levels of MUP following v2.2 infection compared to v54-infected or uninfected controls ($P = 0.10^{-9}$). There were nonsignificant (ns) differences between v54-infected mice and uninfected controls ($P \geq 0.4$). Significance is $^{***}P < 0.0001$. (*D*) Results of qPCR demonstrates MUP transcription took place in the liver and not kidney. Transcription of MUP following v2.2 infection was significantly greater (7-fold) than transcription of MUP following v54 infection. (*E*) MUP presence in hepatocytes of the liver (*Top* 3 panels) and in renal tubules (green color) of v2.2 and v54 30 d postinfection of C57BL/6 mouse (*Bottom*). MUP is present in hepatocytes and renal tubules; it is not in DCs, endothelial, or Kupffer cells (see also Fig. 5*A*).

The availability of closely paired viral variants with distinct opposite phenotype—that is, LCMV Cl 13 vs. ARM 53b, UBC aggressive vs. docile strains (26, 29), and now WE v54 vs. v2.2, and v2.2 vs. ARM 53b—offers unique reagents to search for additional cell surface receptors for entry of other Old World arenaviruses, leading to a better understanding of viral pathogenesis, as well as providing data for structural analysis. Such data provided a direct correlation of negligible infection of DCs with a robust generation of effector T cells. Virus-infected DCs release the immunosuppressive molecules IL-10 (10) and express PD-1, PD-1/PD-L1 (34). Thus, interaction of infected DCs in germinal centers with naïve CD8 and CD4 T cells are likely to exhaust these cells and abort their function. This does not occur following infection with v2.2 or ARM 53b, which infects a minimal number of DCs.

The recorded differences between parental ARM and its in vivo tissue-selected lymphoid variant Cl 13 mimic multiple differences between v2.2 and v54, respectively. Variant 2.2 and v54 were selected from in vitro-infected cultured cells. Cl 13, ARM 53b, and v54 have a Ser at GP residue 153, while v2.2 has a Phe at residue 260. Cl 13, v2.2, and v54 have a Leu at GP residue 260, while ARM 53b has a Phe at that spot. The Phe of v2.2 and ARM 53b in virus glycoprotein residues 153 or 260, respectively, prevented binding to the α-DG receptor (11, 15, 17) (Figs. 1 and 2). These single amino acid differences coupled with receptor-binding studies were essential in mapping the likely location of the α-DG binding site in GP trimer (14). Surprisingly, while v2.2 elicited high levels of pheromone, ARM 53b did not. A collection of reagents is now available to dissect and better compare commonality or differences for the molecular mechanism of pheromone production along with receptor binding, entry, T cell exhaustion, and viral persistence.

Importantly, the increased MUP following v2.2 infection is unique as a known report of a virus inducing and influencing pheromones. MUP family are homologs of mouse pheromones (9, 35–37). Changes in MUP levels or selected species like darcin (MUP 20), an 18,893-Da molecule (8, 9), reflect a communication, breeding, and a health survival advantage. We have, in preliminary experiments, identified and sequenced the darcin MUP species in urine from C57BL/6 and FVB/N mice infected with v2.2. A male mouse with high urinary MUP (darcin) would likely preferentially

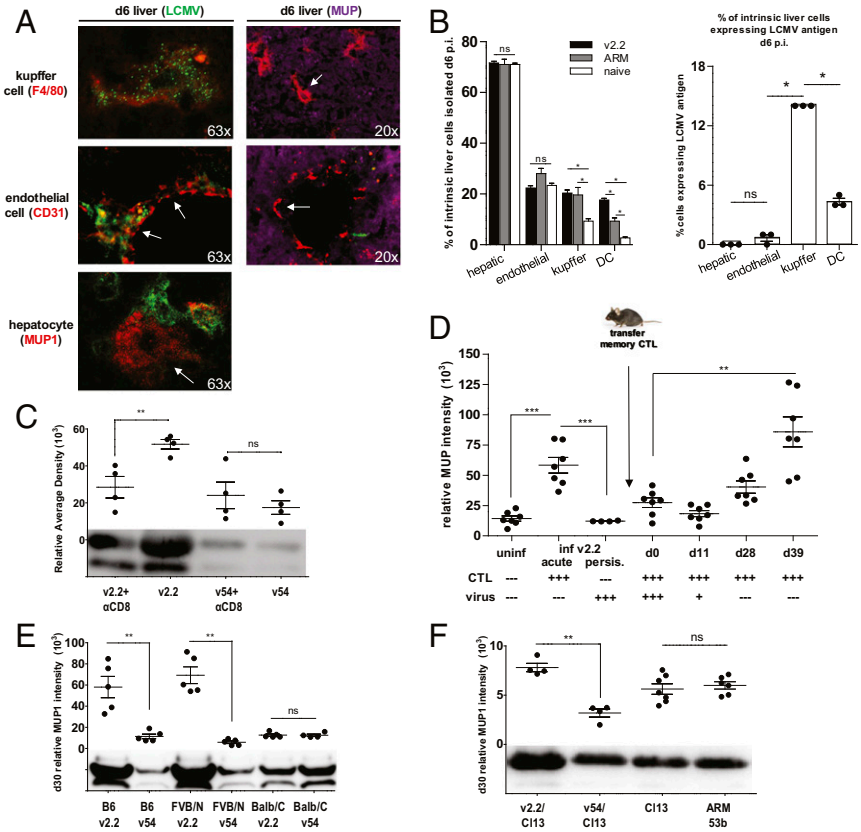

Fig. 5. (*A*) Absence of MUP (red color: arrows) in Kupffer and endothelial cells. Virus (green color) infected primarily Kupffer, low levels of endothelial cells, and also DCs but not hepatocytes (*A* and *B*, *Right*). All mice were male. (*B*, *Left*) Intrinsic hepatic and endothelial cells recovered from v2.2- or ARM 53b-infected or uninfected livers were roughly equivalent. In contrast, fewer Kupffer cells were recovered from uninfected mice than v2.2- or ARM-infected hosts. (*Right*) Presence of LCMV NP antigens in Kupffer, endothelial, or DC cells 6 d after v2.2 infection. (*C*) Deletion of CD8 CTL (a CD8) significantly ($P \leq 0.001$) reduced MUP in the urine of v2.2-infected mice but had no significant (ns) effect on levels of MUP in v54-infected mice. (*D*) Mice persistently infected with v2.2, which lacked functional CD8 CTL, failed to generate MUP. However, when such persistently infected v2.2 mice were reconstituted with virus-specific CTL by adoptive transfer (2×10^8 immune memory T cells) virus was cleared, followed by a robust MUP expression ($P \leq 0.001$). (*E*) Recorded significant MUP expression in urine from C57BL/6 and FVB/N but not Balb mice after infection with v2.2. (*F*) Documented use of chimeric viruses of GP of v2.2 or v54 on Cl 13 backbone. Note that the GP gene of v2.2 and not v54 was involved in expression of MUP. Neither ARM 53b nor Cl 13 infection of C57BL/6 mice significantly enhance urinary MUP levels over that observed with naïve or v54-infected mice. Enhanced exposure (2.5 times) over that used for *D* and *F* were used. Dots in panels indicated values for an individual mouse. $*P < 0.05$; $**P < 0.001$; and $***P < 0.005$.

attract more females for breeding than would a corresponding male with low MUP. The elevated MUP we report here is totally dependent on viral infection (v2.2) and the obligatory CTL response to clear the infection. Such a male would have immune memory T cells and thus be protected from a recurrence of the LCMV pathogen. A possibility we are actively exploring is that these immune-protected/high urine-expressing MUP mice would selectively attract female mice for breeding over males with low urinary MUP. The result being an adoptive behavior-selective advantage as the offspring progeny would be resistant to persistent viral infection. Mice persistently infected with LCMV have health and survival disadvantages (38, 39). This possibility is being explored by mapping sexual behavior in mice. We are also investigating: the role and mechanism of the specific v2.2-induced CTLs; its interaction with virus-infected Kupffer cells, endothelial cells, or DCs; roles—if any—of cytokines and chemokines or other molecules made that induce pheromone production by hepatocytes; and how MUP in the absence of other proteins is secreted into the urine instead of being absorbed by renal tubules.

Materials and Methods

The C57Bl/6, FVB/N, and Balb/cdj mice (6- to 8-wk-old) were obtained from the rodent breeding colony at The Scripps Research Institute. All mice were maintained in pathogen-free conditions and handling conformed to the requirements of the NIH, The Scripps Research Institute Institutional Animal Care and Use Committee, and the Assessment and Accreditation of Laboratory Animal Care. See *SI Appendix* for more detailed materials and methods.

ACKNOWLEDGMENTS. This is Pub. No. 29680 from The Scripps Research Institute, La Jolla, CA. We thank Alexa Murray for technical assistance and Gay Wilkins-Blade for manuscript preparation. This work was supported by NIH Grants AI009484 and AI099699 (to M.B.A.O.), NIH Training Grant T32 AI007036 (to S.L.), The Jeanette Bertea Hennings Foundation (B.S.M.), and in part by Paul D. Wellstone Muscular Dystrophy Cooperative Research Center Grant 1U54 NS053672 (to K.P.C.). K.P.C. is an investigator of the Howard Hughes Medical Institute.

1. F. J. Dutko, M. B. A. Oldstone, Genomic and biological variation among commonly used lymphocytic choriomeningitis virus strains. *J. Gen. Virol.* **64**, 1689–1698 (1983).
2. T. M. Rivers, T. F. Scott, Meningitis in man caused by a filterable virus: II. Identification of the etiological agent. *J. Exp. Med.* **63**, 415–432 (1936).
3. J. Buesa-Gomez, M. N. Teng, C. E. Oldstone, M. B. A. Oldstone, J. C. de la Torre, Variants able to cause growth hormone deficiency syndrome are present within the disease-nil WE strain of lymphocytic choriomeningitis virus. *J. Virol.* **70**, 8988–8992 (1996).
4. M. N. Teng, P. Borrow, M. B. A. Oldstone, J. C. de la Torre, A single amino acid change in the glycoprotein of lymphocytic choriomeningitis virus is associated with the ability to cause growth hormone deficiency syndrome. *J. Virol.* **70**, 8438–8443 (1996).
5. M. N. Teng, M. B. A. Oldstone, J. C. de la Torre, Suppression of lymphocytic choriomeningitis virus-induced growth hormone deficiency syndrome by disease-negative virus variants. *Virology* **223**, 113–119 (1996).

6. M. J. Buchmeier, J. C. de la Torre, C. J. Peters, "Arenaviridae: The viruses and their replication" in *Fields Virology*, D. Knipe, P. Howley, Eds. (Lippincott Williams and Wilkins, Philadelphia, PA, ed. 5, 2007), pp. 1791–1828.
7. Y. Riviere, R. Ahmed, P. Southern, M. B. A. Oldstone, Perturbation of differentiated functions during viral infection in vivo. II. Viral reassortants map growth hormone defect to the S RNA of the lymphocytic choriomeningitis virus genome. *Virology* **142**, 175–182 (1985).
8. S. A. Roberts, A. J. Davidson, L. McLean, R. J. Beynon, J. L. Hurst, Pheromonal induction of spatial learning in mice. *Science* **338**, 1462–1465 (2012).
9. S. A. Roberts *et al*., Individual odour signatures that mice learn are shaped by involatile major urinary proteins (MUPs). *BMC Biol.* **16**, 48 (2018).
10. C. T. Ng, M. B. A. Oldstone, Infected CD8α- dendritic cells are the predominant source of IL-10 during establishment of persistent viral infection. *Proc. Natl. Acad. Sci. U.S.A.* **109**, 14116–14121 (2012).
11. M. B. A. Oldstone, K. P. Campbell, Decoding arenavirus pathogenesis: Essential roles for alpha-dystroglycan-virus interactions and the immune response. *Virology* **411**, 170–179 (2011).
12. N. Sevilla *et al*., Immunosuppression and resultant viral persistence by specific viral targeting of dendritic cells. *J. Exp. Med.* **192**, 1249–1260 (2000).
13. W. Cao *et al*., Identification of alpha-dystroglycan as a receptor for lymphocytic choriomeningitis virus and Lassa fever virus. *Science* **282**, 2079–2081 (1998).
14. K. M. Hastie *et al*., Crystal structure of the prefusion surface glycoprotein of the prototypic arenavirus LCMV. *Nat. Struct. Mol. Biol.* **23**, 513–521 (2016).
15. S. Kunz, N. Sevilla, D. B. McGavern, K. P. Campbell, M. B. A. Oldstone, Molecular analysis of the interaction of LCMV with its cellular receptor [alpha]-dystroglycan. *J. Cell Biol.* **155**, 301–310 (2001).
16. S. C. Smelt *et al*., Differences in affinity of binding of lymphocytic choriomeningitis virus strains to the cellular receptor alpha-dystroglycan correlate with viral tropism and disease kinetics. *J. Virol.* **75**, 448–457 (2001).
17. B. M. Sullivan *et al*., Point mutation in the glycoprotein of lymphocytic choriomeningitis virus is necessary for receptor binding, dendritic cell infection, and long-term persistence. *Proc. Natl. Acad. Sci. U.S.A.* **108**, 2969–2974 (2011).
18. R. Ahmed, M. B. A. Oldstone, Organ-specific selection of viral variants during chronic infection. *J. Exp. Med.* **167**, 1719–1724 (1988).
19. D. P. Berger, D. Homann, M. B. A. Oldstone, Defining parameters for successful immunocytotherapy of persistent viral infection. *Virology* **266**, 257–263 (2000).
20. J. N. Blattman, D. J. Sourdive, K. Murali-Krishna, R. Ahmed, J. D. Altman, Evolution of the T cell repertoire during primary, memory, and recall responses to viral infection. *J. Immunol.* **165**, 6081–6090 (2000).
21. M. Matloubian, R. J. Concepcion, R. Ahmed, CD4+ T cells are required to sustain CD8+ cytotoxic T-cell responses during chronic viral infection. *J. Virol.* **68**, 8056–8063 (1994).
22. A. Tishon, H. Lewicki, G. Rall, M. Von Herrath, M. B. A. Oldstone, An essential role for type 1 interferon-gamma in terminating persistent viral infection. *Virology* **212**, 244–250 (1995).
23. R. M. Zinkernagel, A. Althage, Antiviral protection by virus-immune cytotoxic T cells: Infected target cells are lysed before infectious virus progeny is assembled. *J. Exp. Med.* **145**, 644–651 (1977).
24. Y. Zhou, L. Jiang, L. Rui, Identification of MUP1 as a regulator for glucose and lipid metabolism in mice. *J. Biol. Chem.* **284**, 11152–11159 (2009).
25. Y. S. Bae, J. W. Yoon, Determination of diabetogenicity attributable to a single amino acid, Ala776, on the polyprotein of encephalomyocarditis virus. *Diabetes* **42**, 435–443 (1993).
26. M. Chen *et al*., Genomic and biological characterization of aggressive and docile strains of lymphocytic choriomeningitis virus rescued from a plasmid-based reverse-genetics system. *J. Gen. Virol.* **89**, 1421–1433 (2008).
27. B. Dietzschold *et al*., Characterization of an antigenic determinant of the glycoprotein that correlates with pathogenicity of rabies virus. *Proc. Natl. Acad. Sci. U.S.A.* **80**, 70–74 (1983).
28. E. Domingo, C. Perales, Quasispecies and virus. *Eur. Biophys. J.* **47**, 443–457 (2018).
29. C. J. Pfau, J. K. Valenti, S. Jacobson, D. C. Pevear, Cytotoxic T cells are induced in mice infected with lymphocytic choriomeningitis virus strains of markedly different pathogenicities. *Infect. Immun.* **36**, 598–602 (1982).
30. M. Salvato, P. Borrow, E. Shimomaye, M. B. A. Oldstone, Molecular basis of viral persistence: A single amino acid change in the glycoprotein of lymphocytic choriomeningitis virus is associated with suppression of the antiviral cytotoxic T-lymphocyte response and establishment of persistence. *J. Virol.* **65**, 1863–1869 (1991).
31. M. Sitbon *et al*., Substitution of leucine for isoleucine in a sequence highly conserved among retroviral envelope surface glycoproteins attenuates the lytic effect of the Friend murine leukemia virus. *Proc. Natl. Acad. Sci. U.S.A.* **88**, 5932–5936 (1991).
32. S. Szepanski, H. J. Gross, R. Brossmer, H.-D. Klenk, G. Herrler, A single point mutation of the influenza C virus glycoprotein (HEF) changes the viral receptor-binding activity. *Virology* **188**, 85–92 (1992).
33. S. Kunz, N. Sevilla, J. M. Rojek, M. B. A. Oldstone, Use of alternative receptors different than alpha-dystroglycan by selected isolates of lymphocytic choriomeningitis virus. *Virology* **325**, 432–445 (2004).
34. T. S. Lim *et al*., PD-1 expression on dendritic cells suppresses $CD8^+$ T cell function and antitumor immunity. *Oncoimmunology* **5**, e1085146 (2015).
35. A. Cavaggioni, C. Mucignat, R. Tirindelli, Pheromone signalling in the mouse: Role of urinary proteins and vomeronasal organ. *Arch. Ital. Biol.* **137**, 193–200 (1999).
36. F. Papes, D. W. Logan, L. Stowers, The vomeronasal organ mediates interspecies defensive behaviors through detection of protein pheromone homologs. *Cell* **141**, 692–703 (2010).
37. L. Stowers, S. D. Liberles, State-dependent responses to sex pheromones in mouse. *Curr. Opin. Neurobiol.* **38**, 74–79 (2016).
38. L. H. Gold *et al*., Behavioral effects of persistent lymphocytic choriomeningitis virus infection in mice. *Behav. Neural Biol.* **62**, 100–109 (1994).
39. M. B. A. Oldstone, Rous-Whipple Award Lecture. Viruses and diseases of the twenty-first century. *Am. J. Pathol.* **143**, 1241–1249 (1993).

PNAS
www.pnas.org

Supplementary Information for

A unique variant of lymphocytic choriomeningitis virus that induces pheromone binding protein MUP: Critical role for CTL

Brian C. Ware[a,1], Brian M. Sullivan[a,1], Stephanie LaVergne[a], Brett S. Marro[a], Toru Egashira[b], Kevin P. Campbell[b], John Elder[c], and Michael B.A. Oldstone[a,*]

Michael B.A. Oldstone, M.D.
Email: mbaobo@scripps.edu

This PDF file includes:

www.pnas.org/cgi/doi/10.1073/pnas.1907070116

Supplementary Information Text

Materials and Methods

Mice and Viruses. C57Bl/6, FVB/N, and Balb/cdj mice (6- to 8-week-old) were obtained from the rodent breeding colony at The Scripps Research Institute (TSRI). All mice were maintained in pathogen-free conditions and handling conformed to the requirements of the NIH, TSRI Institutional Animal Care and Use Committee, and AAALAC. Except for MUP urinary studies which utilized only males, groups of four to six male and female mice were used throughout with equivalent results. With MUP analysis in v2.2 and v54 infected C57Bl/6 mice only males in groups of 20 or more mice were used. Experiments were repeated two to four times. Newborn mice were obtained by breeding and were inoculated with 1×10^3 PFU of virus i.c. within 18 hrs. following birth. v54, v2.2, LCMV Cl 13 and ARM 53b were obtained, grown, stored and quantified by plaque assay according to previously published methods (1-9). Adult mice were infected by i.v. injection of 2×10^6 PFU of the various viruses and newborn mice i.c. with 10^3 PFU of virus. For quantitation of viremia, blood was drawn from the retro-orbital sinus under isoflurane anesthesia. To determine virus load in tissues, tissues were harvested from euthanized mice and frozen at -80°C. At time of infectious assay, tissues were thawed, weighed and homogenized in sterile media (5% FCS) w/v, clarified by low-speed centrifugation and resultant supernatant plaqued.

Cytotoxic T Cell and Dendritic Cell/FACs Assays. A ^{51}Cr release assay, peptide stem/FACS assay and tetramer studies were performed as previously reported (1, 2, 5, 8, 10-12). Separation, staining and FACS analysis has been reported (8, 11, 12). Deletion of host CD8 CTL utilized monoclonal antibody YTS.1694 as reported in our previous publications (2, 9, 11, 12). Generation of memory CD8 CTL and transfer of 2×10^7 T cells into persistently infected mice has been reported (2, 9).

Specialized ESCs, Antibody Reagents and Treatments. ESCs expressing α-DG or not were a gift from K.P. Campbell and grown as reported (13, 14). Mouse monoclonal antibody (IIH-6) to α-DG was obtained from K.P. Campbell, made and used as reported (13, 14). Antibody VL4 to LCMV v2.2, v54, Cl 13 and ARM 53b NP was purchased from BioXCell and used as reported (15). Guinea pig antibody to LCMV was raised, generated and used as published (15, 16). Antibodies used for immunohistochemical staining of liver tissues for endothelial cells or DCs were CD31 (BioLegend) or F4/80 (Abcam), respectively. Staining for MUP in liver and kidney used rabbit antibody to mouse MUP (Abcam).

Virus Overlay Protein Blot Assay and ELISA. Reagents and procedures used have been reported (5, 10, 13, 17, 18).

Immunohistochemistry, Flow Cytometry, and Western Blots. Mice were perfused intracardially with 10 ml of PBS. Samples of liver were excised and snap-frozen in OCT on dry ice with 100% ethanol. Frozen tissues were sectioned at 10 µm on cryotome, placed on glass slides, vacuum dehydrated for 10 min and stored at -80°C in a dehydrated slide box. Upon removal from -80°C, slides were immediately placed into 4% PFA for 15 min, then blocked using 50 µl of 10% milk in PBS for 2 hr. at room temperature. After washing 1x in PBS, primary antibodies (rabbit anti-mouse MUP1 or guinea pig anti-LCMV) added in a 1:100 dilution in 50 µl (10% milk + PBS) at room temperature for 1 hr. Sections were washed 3x in PBS for 10 min, secondary (anti-rabbit IgG Alexa Fluor 488, or anti-guinea pig IgG Alexa Fluor 555, respectively) added at 1:200 dilution (10% milk + PBS) for 30 min. Slides were again washed 3x, dried, 10 µl of DAPI mount (Southern Biotech 0100-20) was added per section and coverslip

applied. Procedure for indirect labeling or use of two or three antibodies on a single section have been reported (15). Tissues were imaged using high resolution confocal microscopy.

Alternatively, to obtain a single cell suspension, liver was perfused as above, excised, diced in collagenase buffer and incubated for 30 min at 37°C. Tissue was transferred to a 100um filter, mashed with the back of a 3ml syringe and rinsed twice with 10ml of RPMI. Samples were spun (1500RPM/4°C/5min), pellets resuspended in 3ml ACK lysis buffer for 1min at room temperature, neutralized with 7ml PBS with 2% FBS, spun and resuspended in 3ml of PBS with 2% FBS. $2x10^6$ cells per well were stained with a cocktail of antibodies diluted 1:200 for 4°C/45min. DCs MHCII-PerCPCy5.5 (BioLegend cat#107625), PDCA1-PE (BioLegend cat#127103), B220-APC (BD Bioscience cat# 17-0452-83), CD11c-PB (BioLegend cat#117322); Kupffer cells F4/80-PE (BioLegend cat#123110), CD11b-PerCPCy5.5 (BD Bioscience cat#550993), CD68-APC (BioLegend cat#137007); endothelial cells CD31-BV421 (BioLegend cat#102403); hepatocytes MUP1 polyclonal rabbit anti-mouse (Abcam cat#ab95198 at 1:1000 dilution/1hr), anti-rabbit AF647 (ThermoFisher cat#a-21245 at 1:500 dil/1hr). After staining samples were fixed, washed again and run on LSRII using Diva software.

Mouse urine was collected according to method of Roberts (19, 20). Two µl of mouse urine was added to 18 µl of PBS + 4 µl of 6x sample buffer and heated at 70°C for 20 min. Samples were spun, and 15 µl/sample was run using Mini-PROTEAN TGX 4-20% 10-well (BioRad, cat# 4561093) in 1x Tris-Glycine buffer at room temperature for 30 min at 200V. PVDF membranes were presoaked in Methanol (Fisher) and transferred to 20 ml of transfer buffer (25 mM Tris, 20 mM glycine, 0.1% SDS, 20% Methanol). Acrylamide gels were removed from cassette and transferred to 20 ml of transfer buffer. Gel and membrane were allowed to equilibrate at room temperature for 5 min before proceeding to assembly, and running at 4°C, 30 min, 95V in transfer apparatus (BioRad). Membrane was then transferred to blocking buffer (5% powdered milk in PBS) for 1 hr. at room temperature. Blocking buffer was decanted, 5% milk

PBST containing rabbit anti-mouse MUP1 (1:2000) was added, incubated overnight at 4°C with constant rocking. Blot was washed in PBS with 0.02% Tween-20 3x 10 min. Secondary anti-rabbit HRP was added at 1:10,000 in 5% milk PBST for 1 hr. Wash step was repeated, membrane transferred to a clear sheet protector. One ml of Thermo WEST pico substrate was added to blot and allowed to incubate for 1-2 min. Blots were imaged using ImageQuant LAS 4000.

QT-PCR for MUP. Livers and kidneys from mice were harvested and immediately frozen. Tissues were dissolved in 1 ml: 100 mg in Trizol reagent (15596018, Thermo) and homogenized for 2 min. with zircon beads. RNA extraction was conducted according to Trizol protocol. Briefly, 1/5 volume of chloroform was added to homogenate, mixed thoroughly and allowed to partially separate for 5 min at room temperature. Homogenates were spun at 13,000 RPM for 10 min. at 4°C. Aqueous layer was delicately transferred to a new tube where it was precipitated, washed 3x with 70% ethanol and dried before resuspension in DEPC-treated water. RNA was quantified, and first strand cDNA was processed by SuperScript III kit. mRNA transcript level was measured using SYBR green QPCR kit. QT-PCR primer sequence for MUP1 was obtained from Zhou's group (21).

Forward primer MUP1: CAAAACAGAAAAGGCTGGTGA

Reverse primer MUP1: TTGTGCAAACCTTTCCTTGA

Biochemical and Histological Analysis of Liver Disease. Hepatocellular injury was monitored by measuring serum alanine amino transferase (ALT) activity (22) (Sigma). Results were expressed as mean serum ALT activity $\pm$ SEM. Tissue samples were fixed in 10% zinc buffered formalin and processed as reported (22).

Statistical Analysis. Group comparisons were analyzed by ANOVA in the Prism software package. Experiments were performed two to four times to insure reproducibility. $P < 0.05$ was considered significant.

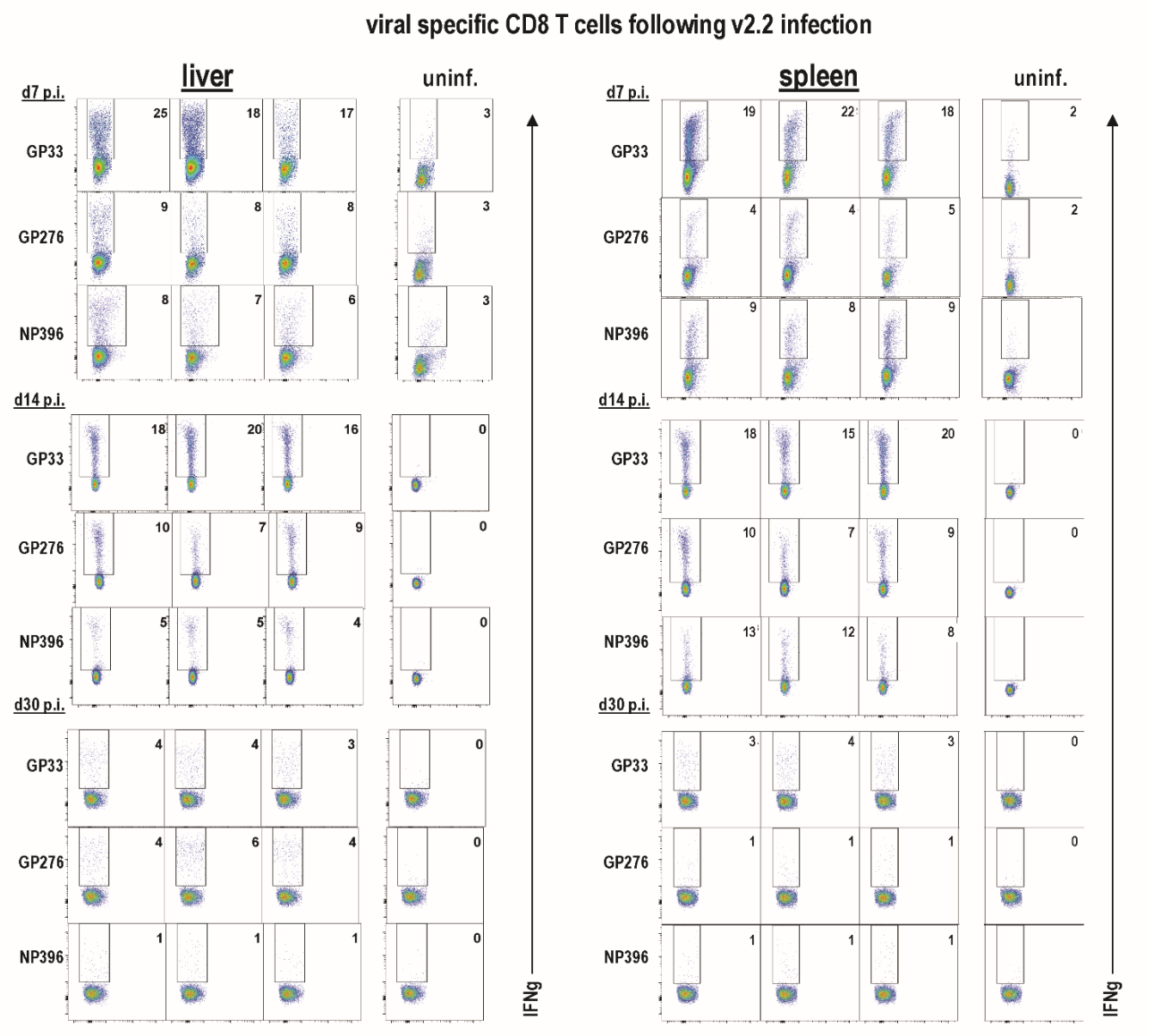

Fig. S1. Quantification of virus-specific CD8 T cells entering the liver or spleen day 7, 14, and 30 post-v2.2 inoculation ($2x10^6$ i.v.) of C57Bl/6 7- to 8-week-old mice.

Viral titers

C57BL/6 mice infected with $2x10^6$PFU i.v. of	d5	d30			
	sera	sera	kidney	liver	urine
v2.2	$5x10^5$	nil	$2x10^3$	nil	nil
v54	$6x10^5$	$7x10^3$	$4x10^5$	$2x10^4$	nil
ARM 53b	$3x10^4$	nil	$5x10^3$	nil	nil
Cl13	$6x10^5$	$4x10^5$	$3x10^5$	$4x10^4$	nil
uninfected	nil	nil	nil	nil	nil

Table S1. Thirty days post infection with v2.2, v54, Cl13, ARM 53b infectious viruses was uniformly found in the kidney but absent from the urine. As anticipated v54 and Cl13 generate a persistent infection measured at day 30 while v2.2 and ARM53b cleared virus from tissues studied.

References

1. Ahmed R & Oldstone MBA (1988) Organ-specific selection of viral variants during chronic infection. *J. Exp. Med.* 167(5):1719-1724.
2. Berger DP, Homann D, & Oldstone MBA (2000) Defining parameters for successful immunocytotherapy of persistent viral infection. *Virology* 266(2):257-263.
3. Buesa-Gomez J, Teng MN, Oldstone CE, Oldstone MBA, & de la Torre JC (1996) Variants able to cause growth hormone deficiency syndrome are present within the disease-nil WE strain of lymphocytic choriomeningitis virus. *J. Virol.* 70(12):8988-8892.
4. Dutko FJ & Oldstone MBA (1983) Genomic and biological variation among commonly used lymphocytic choriomeningitis virus strains. *J. Gen. Virol.* 64:1689-1698.
5. Sevilla N, *et al.* (2000) Immunosuppression and resultant viral persistence by specific viral targeting of dendritic cells. *J. Exp. Med.* 192(9):1249-1260.
6. Teng MN, Borrow P, Oldstone MBA, & de la Torre JC (1996) A single amino acid change in the glycoprotein of lymphocytic choriomeningitis virus is associated with the ability to cause growth hormone deficiency syndrome. *J. Virol.* 70(12):8438-8443.
7. Teng MN, Oldstone MBA, & de la Torre JC (1996) Suppression of lymphocytic choriomeningitis virus--induced growth hormone deficiency syndrome by disease-negative virus variants. *Virology* 223(1):113-119.
8. Ng CT & Oldstone MBA (2012) Infected CD8alpha- dendritic cells are the predominant source of IL-10 during establishment of persistent viral infection. *Proc. Natl. Acad. Sci. USA* 109(35):14116-14121.
9. Tishon A, Lewicki H, Rall G, von Herrath M, & Oldstone MBA (1995) An essential role for type 1 interferon-gamma in terminating persistent viral infection. *Virology* 212(1):244-250.
10. Smelt SC, *et al.* (2001) Differences in affinity of binding of lymphocytic choriomeningitis virus strains to the cellular receptor alpha-dystroglycan correlate with viral tropism and disease kinetics. *J. Virol.* 75(1):448-457.
11. Sullivan BM, *et al.* (2011) Point mutation in the glycoprotein of lymphocytic choriomeningitis virus is necessary for receptor binding, dendritic cell infection, and long-term persistence. *Proc. Natl. Acad. Sci. USA* 108(7):2969-2974.
12. Teijaro JR, *et al.* (2013) Persistent LCMV infection is controlled by blockade of type I interferon signaling. *Science* 340:207-211.
13. Cao W, *et al.* (1998) Identification of alpha-dystroglycan as a receptor for lymphocytic choriomeningitis virus and Lassa fever virus. *Science* 282(5396):2079-2081.
14. Henry MD & Campbell KP (1998) A role for dystroglycan in basement membrane assembly. *Cell* 95(6):859-870.
15. Marro BS, *et al.* (2017) Progression of type 1 diabetes from the prediabetic stage is controlled by interferon-alpha signaling. *Proc. Natl. Acad. Sci. USA* 114(14):3708-3713.

16. Welsh RM, Lampert PW, Burner PA, & Oldstone MBA (1976) Antibody-complement interactions with purified lymphocytic choriomeningitis virus. *Virology* 73(1):59-71.
17. Hastie KM, *et al.* (2016) Crystal structure of the prefusion surface glycoprotein of the prototypic arenavirus LCMV. *Nat. Struct. Mol. Biol.* 23(6):513-521.
18. Kunz S, Sevilla N, McGavern DB, Campbell KP, & Oldstone MBA (2001) Molecular analysis of the interaction of LCMV with its cellular receptor [alpha]-dystroglycan. *J. Cell Biol.* 155(2):301-310.
19. Roberts SA, Davidson AJ, McLean L, Beynon RJ, & Hurst JL (2012) Pheromonal induction of spatial learning in mice. *Science* 338:1462-1465.
20. Roberts SA, *et al.* (2018) Individual ordour signatures that mice learn are shaped by involatile major urinary proteins (MUPs). *BMC Biology* 16:48.
21. Zhou Y, Jiang L, & Rui L (2009) Identification of MUP1 as a regulator for glucose and lipid metabolism in mice. *J. Biol. Chem.* 284(17):11152-11159.
22. Guidotti LG, *et al.* (1996) Viral cross talk: Intracellular inactivation of the hepatitis B virus during an unrelated viral infection of the liver. *Proc. Natl. Acad. Sci. USA* 93:4589-4594.